







Article

In Silico Contact Pressure of Metal-on-Metal Total Hip Implant with Different Materials Subjected to Gait Loading

J. Jamari ^{1,2}, Muhammad Imam Ammarullah ^{2,3,4,*}, Gatot Santoso ^{3,4}, S. Sugiharto ^{3,4}, Toto Supriyono ^{3,4}
and Emile van der Heide ⁵

- ¹ Department of Mechanical Engineering, Faculty of Engineering, Diponegoro University, Semarang 50275, Central Java, Indonesia; j.jamari@gmail.com
- ² Undip Biomechanics Engineering & Research Centre (UBM-ERC), Diponegoro University, Semarang 50275, Central Java, Indonesia
- ³ Department of Mechanical Engineering, Faculty of Engineering, Pasundan University, Bandung 40153, West Java, Indonesia; gatot.santoso@unpas.ac.id (G.S.); sugih.sugiharto@unpas.ac.id (S.S.); supriyono.toto@unpas.ac.id (T.S.)
- ⁴ Biomechanics and Biomedics Engineering Research Centre, Pasundan University, Bandung 40153, West Java, Indonesia
- ⁵ Laboratory for Surface Technology and Tribology, Faculty of Engineering Technology, University of Twente, P.O. Box 217, 7500 AE Enschede, The Netherlands; e.vanderheide@utwente.nl
- * Correspondence: imamammarullah@gmail.com; Tel.: +62-895-3359-22435

Abstract: The use of material for implant bearing has a vital role in minimizing failures that endanger implant recipients. Evaluation of contact pressure of bearing material can be the basis for material selection and have correlations with wear that contribute to the need of revision operations. The current paper aims to investigate three different metallic materials, namely cobalt chromium molybdenum (CoCrMo), stainless steel 316L (SS 316L), and titanium alloy (Ti6Al4V) for application in metal-on-metal bearing of total hip implant in terms of contact pressure. In silico model based on finite element simulation has been considered to predict contact pressure of metal-on-metal bearings under normal walking conditions. It is found that the use of Ti6Al-4V-on-Ti6Al4V is superior in its ability to reduce contact pressure by more than 35% compared to the other studied metal-on-metal couple bearings.

Keywords: contact pressure; gait; in silico; metal-on-metal; total hip implant



Citation: Jamari, J.; Ammarullah, M.I.; Santoso, G.; Sugiharto, S.; Supriyono, T.; van der Heide, E. In Silico Contact Pressure of Metal-on-Metal Total Hip Implant with Different Materials Subjected to Gait Loading. *Metals* **2022**, *12*, 1241. <https://doi.org/10.3390/met12081241>

Academic Editors: Uroš Župerl and Irina P. Semenova

Received: 20 June 2022

Accepted: 19 July 2022

Published: 23 July 2022

Publisher's Note: MDPI stays neutral with regard to jurisdictional claims in published maps and institutional affiliations.



Copyright: © 2022 by the authors. Licensee MDPI, Basel, Switzerland. This article is an open access article distributed under the terms and conditions of the Creative Commons Attribution (CC BY) license (<https://creativecommons.org/licenses/by/4.0/>).

1. Introduction

In the field of orthopedics, surgical replacement of diseased human hip joints, such as osteolysis, has been successfully performed using total hip implants [1–3]. The use of hard-on-soft bearings, such as metal-on-polyethylene and ceramic-on-polyethylene has generally been implanted in the human system through hip replacement surgery. Unfortunately, the wear particles of the polyethylene material in their articulation with the hard material can result in a reduced life span of the artificial hip joint [4–6]. The wear particles of polyethylene range in size between sub-micrometers to micrometers and can absorb into human bone resulting in mechanical loosening and fixation loss of implant components [7]. Ultimately, reoperation is required to correct the condition with a new hip joint prosthesis.

Hard-on-hard bearings can be a choice for implants due to the disadvantages of hard-on-soft, with the option of using metal or ceramic materials. To avoid revision surgery of hip joint implant recipients with high activity intensity and younger age, the use of metal-on-metal bearings may be considered [8]. This is because ceramic materials have brittle characteristics that endanger patients due to the high risk of failure from fracture caused by various high-intensity activities, generally carried out by younger patients [9]. In addition, compared to conventional metal-on-polyethylene bearings, metal-on-metal bearings produce approximately 200 times lower wear. Although it is not the best bearing

option when viewed from the number of failure cases compared to other bearing options, metal-on-metal is still widely used by surgeons to meet the needs of the national market independently without import in various developing countries, including Indonesia [10]. This is due to the relatively affordable price, ease of production process with limited tools, and ease to obtain raw materials [11].

Metal ions generated from wear particles in metal-on-metal bearings circulate in the body, causing local inflammation and contributing to osteolysis. [12–14]. Metal wear particles can circulate in the lymphatic system far from the prosthesis position and metal deposits are found in the bone marrow, lymph nodes, and liver. The reactive nature of these metal wear particles also has the potential to cause cytotoxicity, hypertension, and neoplasia. To solve this problem, the proper selection of the metal material needs to be evaluated further due to concerns regarding biological problems to minimize failures that occur. Metal materials commonly used as bearing materials include cobalt chromium molybdenum (CoCrMo) [15], stainless steel 316 L (SS 316L) [16], and titanium alloy (Ti6Al4V) [17]. In the development of implants that are suitable for the Indonesian population and most countries in Asia as developing countries, apart from looking at the material aspect, the size of the implant also needs to be considered. The geometry of total hip implants available in the market as well as various current studies refer to European sizes that are different from Asian sizes. A metal-on-metal total hip implant that adopts Indonesian geometries needs to be established.

Several studies in the development of medical implant have been carried out in vitro [18], in vivo [19], and in silico [20]. Adoption in silico becomes a rational option as an initial study before conducting long-term inversion, either in vitro or in vivo. In addition to being able to save time, in silico research also does not require relatively costly laboratory test equipment as in vitro and approval of research involving living organisms to completion as in vivo. With the demands of development and innovation in the medical and pharmaceutical sectors, more studies are being conducted on computers to solve problems that approximate the results from in vitro and in vivo. The extraordinary capabilities of in silico research have the potential to revolutionize knowledge in the medical and pharmaceutical sectors, such as the study of total hip implants.

The evaluation of contact pressure on implants as a preliminary study was extensively carried out in previous studies before the evolution of wear [21–23]. This is because contact pressure has a correlation with wear according to the Archard wear equation [24] as shown in Equation (1), where W_L is linear wear, K_w is wear coefficient, P is contact pressure, and s is sliding distance. Based on this equation, contact pressure has a linear correlation with linear wear. This means, reducing wear can be achieved by reducing contact pressure.

$$W_L = K_w P s \quad (1)$$

Apart from the Archard wear equation which proved that wear can be minimized by reducing the magnitude of contact pressure, other evidence is also demonstrated through the experimental testing from Levanov et al. [25]. The results of this study explain the correlation between intensity of wear and contact pressure, where it is found that the intensity of wear tends to increase with increasing contact pressure. Correlation of intensity of wear and contact pressure from the results of Levanov et al. [25] is described in Figure 1.

Some research computational studies have been conducted on metallic bearing in total hip implants. De la Torre et al. [26] studied von Mises stress from CoCrMo femoral head against ultra-high molecular weight polyethylene (UHMWPE) acetabular cup with cemented and uncemented configuration. Furthermore, Jamari et al. [27] evaluate contact pressure on metal-on-polyethylene bearing with different femoral head materials under the gait cycle. Moreover, Ammarullah et al. [28] investigate Tresca stress of UHMWPE acetabular cup with a counterpart of CoCrMo femoral head during loads based on six different types of body mass index categories. Using a commercially pure titanium femoral head connecting with UHMWPE acetabular cup, Handoko et al. [29] investigate wear volume with different femoral head diameters of 0.5 mm, 1 mm, and 1.25 mm. Though

a metallic head together with different plastic liner was studied in the past, metal-on-metal bearing couples with three commonly used materials such as CoCrMo, SS 316L, and Ti6Al4V that are mostly used in developing countries were less reported. In addition, the use of geometry for the Indonesian population is also still rarely performed.

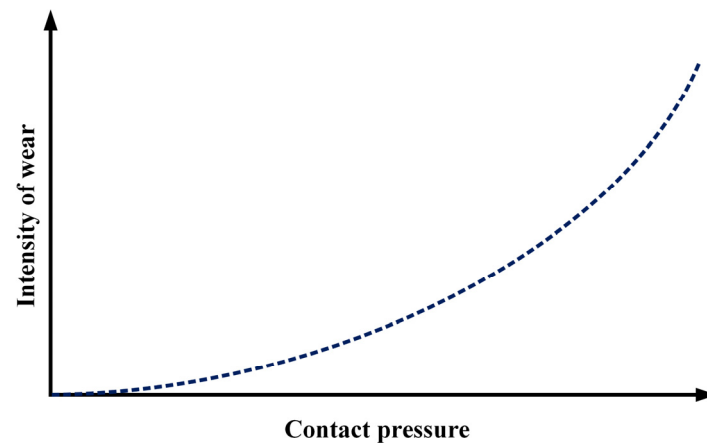


Figure 1. Correlation between contact pressure and intensity of wear [25].

The purpose of this study is to analyze the contact pressure of bearing metal-on-metal total hip implant with different materials, namely CoCrMo, SS 316L, and Ti6Al4V using Indonesian hip joint geometry. We used in silico model based on finite elements to complete the contact pressure prediction in this paper with a gait condition that refers to the physiological activity of the human hip joint.

2. Materials and Methods

2.1. Bearing Geometry and Materials

An acetabular cup of 5 mm thickness and femoral head of 28 mm diameter are used for geometry of total hip implant with 50 μm radial clearance as adopted based on patient's hip joint geometry from Indonesia and countries in Asia [30]. For material properties, Young's modulus for CoCrMo is 210 GPa, SS 316L is 193 GPa, and Ti6Al4V is 110 GPa [31], while the Poisson ratio is 0.3 for all materials assuming homogeneity, isotropic, and linear elasticity. Coefficient of friction for metal-on-metal bearing that used CoCrMo, SS 316L, and Ti6Al4V used the same materials in both femoral head and acetabular cup are 0.2, 0.8, and 1 [31], respectively.

2.2. In Silico Model

Finite element simulation for in silico metal-on-metal model running with ABAQUS/CAE 6.14-1 (Dassault Systèmes, Vélizy-Villacoublay, France) is represented by two main components, acetabular cup and femoral head. In the definition of contact between surfaces, the master surface is the contacting femoral head surface and the slave surface is the contacting acetabular cup surface. We adopted a 2D ball-in-socket model with an asymmetry forming a quarter circle that did not consider the pelvic bone component in the simulation to speed up the time required to complete the computational simulation. This is because it did not significantly affect the results [32]. The optimum number of elements for our finite element model is 5500 consisting of 2000 CAX4 for the acetabular cup and 3500 CAX4 for the femoral head. The finite element model we used is explained in Figure 2.

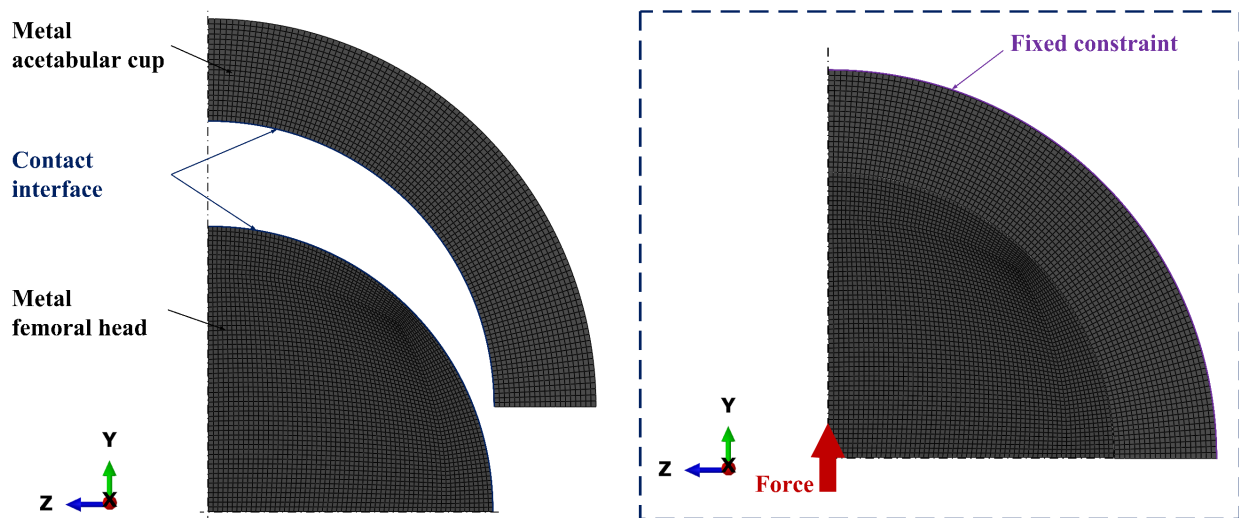


Figure 2. In silico model of metal-on-metal bearing couple.

2.3. Gait Loading

Patients who have undergone hip joint replacement surgery with a total hip implant will carry out gait activities as the most common daily activities. To provide a physiological condition according to the actual condition of the human hip joint, the load is given with a gait condition. We adopted the gait conditions used by Jamari et al. [24] for one cycle that is simplified into 32 phases, but without considering the range of motion as conducted by Basri et al. [33] described in Figure 3. Phases 1–19 are referred to as the ‘stance phase’, which represent the initial 60% of the gait cycle and phases 20–32 are referred to as the ‘swing phase’, which represent the final 40% of the gait cycle.

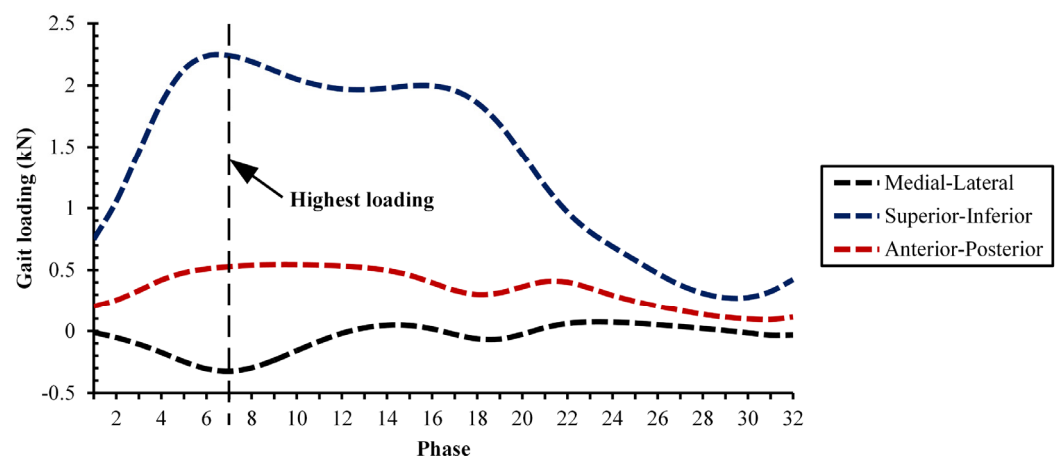


Figure 3. Triaxial forces during gait loading [24].

3. Results and Discussion

Validation needs to be conducted to determine the accuracy of the computational simulation results obtained from published literature under identical conditions, either analytical, computational, clinical, or experimental. In the current work, we compared the maximum contact pressure of metal-on-metal bearings using CoCrMo with published results of Jamari et al. [24] and Hertzian contact (see Equation (2), where F denotes the forces during gait loading, and a is contact radius) [34]. The comparison of maximum contact pressure as validation is described in Figure 4. Jamari et al. [24], and Hertzian contacts [34] change during one gait cycle as the magnitude of the applied triaxial forces change over time. The difference in the maximum contact pressure magnitude below

10% seems to be in the permissible range so it can be said that the computational model developed in this study is valid.

$$\frac{3F}{2\pi a^2} \tag{2}$$

Figure 5 describes the maximum contact pressure for metal-on-metal bearings with a variety of different metal materials in a full cycle under gait loading. As for the comparison of the highest, lowest, and average contact pressures of the maximum contact pressures of the 32 phases described in Figure 6. Because the resultant force changes over time gait cycle, the maximum contact pressure changes in each phase, with the highest contact pressure being in the 7th phase. Of the three types of metal-on-metal bearings in the current study, the contact pressures from the highest to the lowest overall were found in CoCrMo-on-CoCrMo, SS 316L-on-SS 316L, and Ti6Al4V-on-Ti6Al4V. Maximum values of contact pressure for the three different types of metal-on-metal bearings are shown in Table 1.

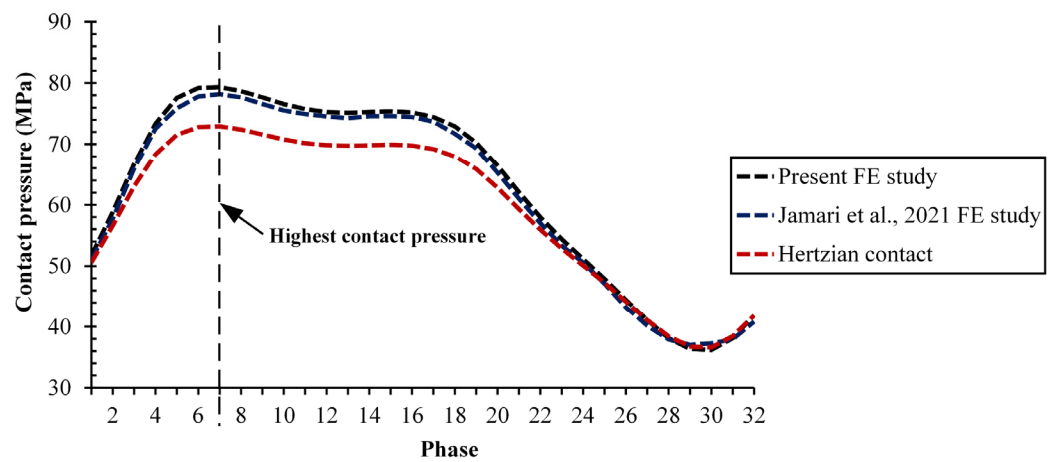


Figure 4. Comparison of the maximum contact pressure with the published results of Jamari et al. [24] and Hertzian contact [34].

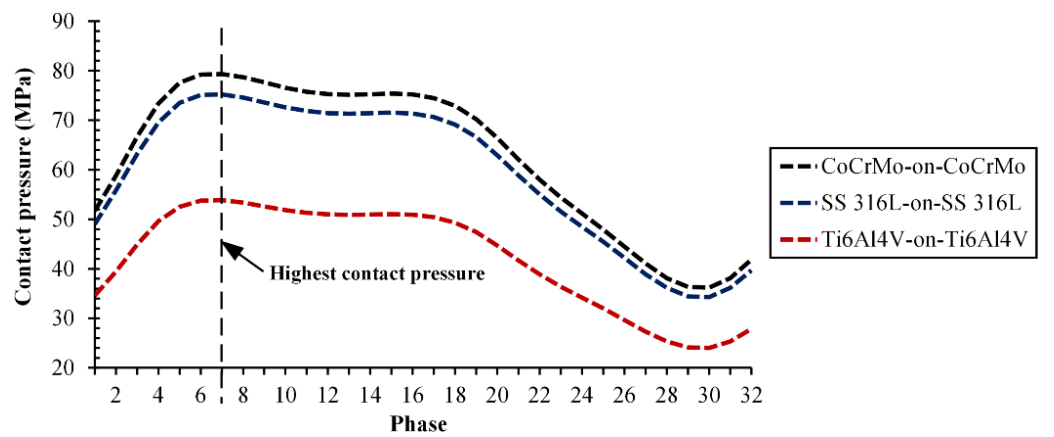


Figure 5. Maximum contact pressure for three types of metal-on-metal bearings.

Table 1. Maximum contact pressure for different metal-on-metal bearing materials at peak loading.

Metal-on-Metal Bearings	Contact Pressure
CoCrMo-on-CoCrMo	79.34 MPa
SS 316L-on-SS 316L	75.23 MPa
Ti6Al4V-on-Ti6Al4V	53.85 MPa

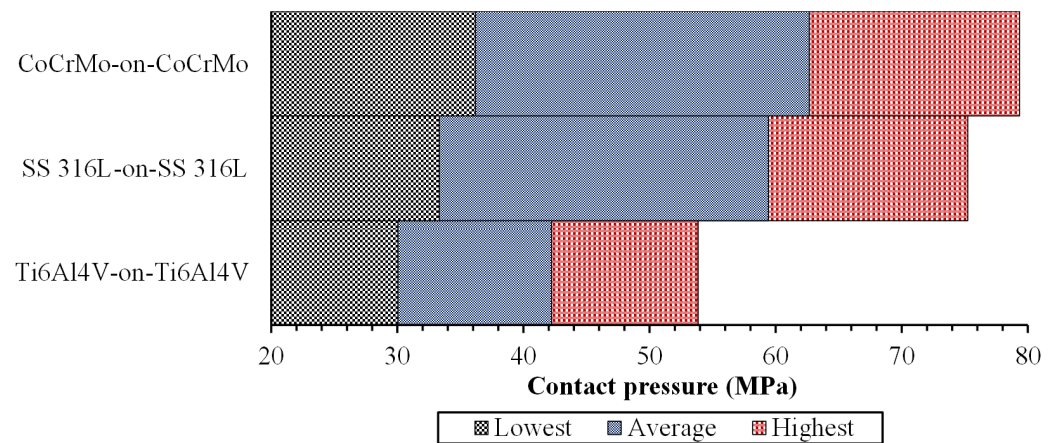


Figure 6. Comparison for the highest, average, and highest contact pressures of the maximum values for all phases.

Meanwhile, the distribution of contact pressure is shown in Figure 7 obtained with the S22 in ABAQUS for the simulation results [35]. A total of five selected phases are taken to explain the contact pressure conditions referred from Jamari et al. [24]. Since micro-separation is not considered during the contact process, the contour of contact pressure is always centered, indicating that no edge contact occurs. However, in actual conditions, edge contact can occur due to various unexpected activities that cause stripe wear [36].

Contact pressure and contact radius relationship on different metal-on-metal bearing materials during peak loading is shown in Figure 8. We can see that contact pressure profiles are different in our simulated metal-on-metal bearings. CoCrMo-on-CoCrMo exhibits the highest contact pressure magnitude compared to other bearings, but the contact radius is only about 3.8 mm during peak loading. On the contrary, Ti6Al4V-on-Ti6Al4V has the lowest contact pressure value compared to other bearings, but the longest contact radius at about 4.7 mm. It is strongly influenced by Young's modulus that gives it a different material hardness affecting the characteristics of the contact [37], where the value of Young's modulus has a linear relationship with the contact pressure, but is inversely proportional to the contact radius.

Archard wear equation [24] as shown in Equation (1) explains that contact pressure has a linear relationship with wear that can cause failure. Despite CoCrMo-on-CoCrMo demonstrating the highest contact pressure, this does not mean that the bearing has the highest wear. This is because based on Archard's wear equation [24], wear is not only affected by contact pressure, but also the wear coefficient that can be obtained through pin-on-disc testing [38]. For initial studies, the contact pressure can be used as a reference for material evaluation to minimize wear failure. However, for further research, it is necessary to conduct wear studies using finite element procedures or hip joint simulators.

In selecting bearing materials for metal-on-metal, apart from the mechanical aspect, we also need to look at the medical aspect. The biggest consideration for not choosing metal-on-metal bearings is the possibility of toxicity due to metal ions. Vara et al. [39] explained that the use of metal materials for orthopedic purposes has several potential negative impacts that endanger implant users and disrupt the performance of various body organs, such as the nervous system, digestive system, immune system, and others. The potential for poisoning by using Ti6Al4V can be minimized from other metal materials due to its better biocompatibility and corrosion resistance when compared to SS 316L and CoCrMo [27].

Looking at the results of the contact pressure study that we performed on material evaluation for metal-on-metal bearings, other efforts to enhance implant ability need to be conducted. Some efforts would be include the application of textured surfaces as explained by Ammarullah et al. [40], as the application of textured surfaces on metal-on-metal bearing could reduce contact pressure. Second, geometric parameters are also important

to investigate as described by Utomo et al. [41] that these parameters may affect implant performance. Next, coating application in implant could minimize medical problems after hip replacement surgery which is in line with Maistrovskaia et al. [42]. Surgical procedures also need to improve since technical issues have implications with failure as explained by London Health Sciences Centre [43] to improve the performance of metal-on-metal bearings in the future. The last, ultra-precision polishing and surface finish on implants also needs to be studied further on metal-on-metal bearings considering the findings of Fan et al. [44–46] and Tian et al. [47] describing its importance for mechanical components.

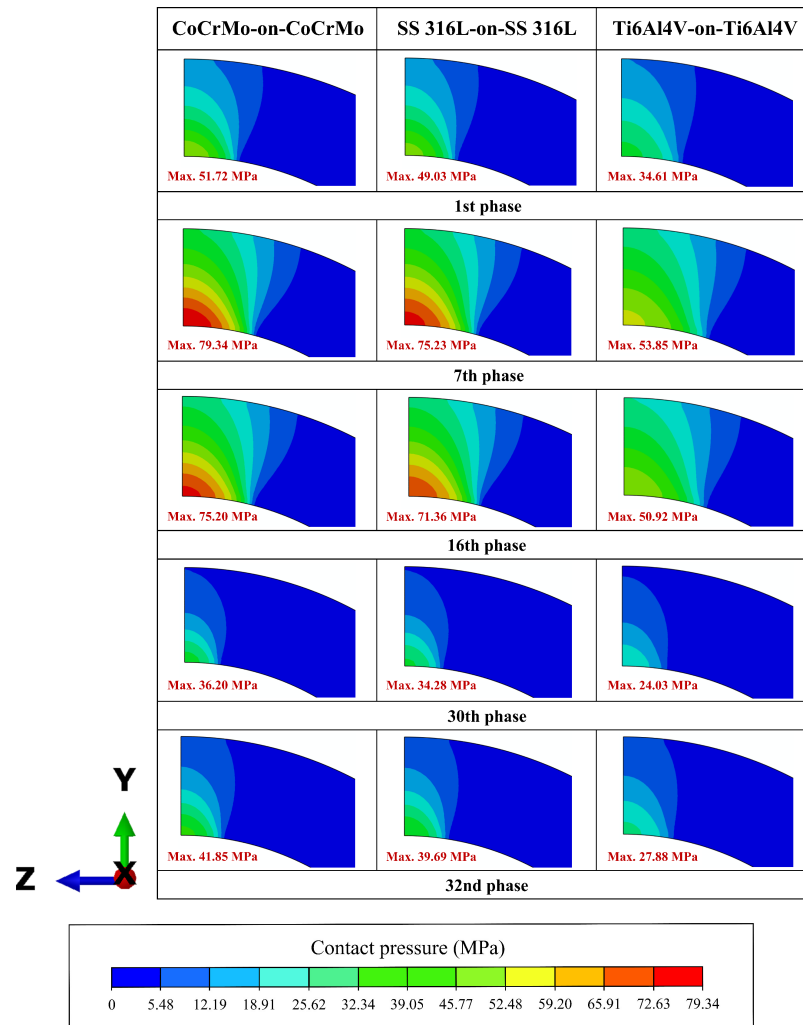


Figure 7. Center position of contact area on metal acetabular cup at selected phases.

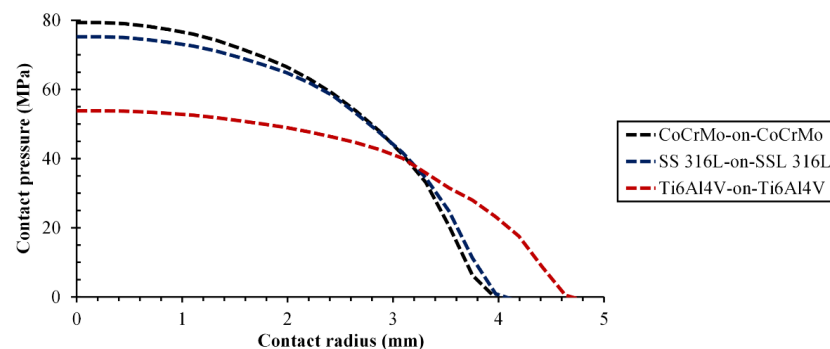


Figure 8. Correlation between contact pressure and contact radius at 7th phase.

In the current computational study, several shortcomings could affect the results. First, the use of friction coefficient under gait conditions only uses a constant coefficient. In fact, the coefficient of friction changes over time according to lubrication conditions, surface roughness, and wear [48]. Furthermore, not accounting for the range of motion and only using vertical loading to load the resultant force does not accurately represent the human physiological condition during the gait process [49]. In addition, our prediction model only considers the components of the femoral head and acetabular cup without considering the fixation system and pelvic bone. Finally, the adoption of an asymmetric 2D finite element model can also reduce the accuracy of the computational results [50]. Various shortcomings in the current research need to be improved in further studies.

4. Conclusions

Contact pressure evaluation for the metal-on-metal bearing of total hip implant using different metallic materials has been successfully investigated using 2D in silico model. An excellent agreement of contact pressure was obtained between the present study, published literature, and Hertzian contact. The highest maximum contact pressure is found in the seventh phase with a similar trend for all simulated metal-on-metal bearings corresponding to the highest resultant force during gait activity. The selection of bearings comprising Ti6Al4V-on-Ti6Al4V demonstrate the best performance to reduce contact pressure, which indicates it has a longer life owing to the reduction in wear. The better biocompatibility and corrosion resistance factors of other bearings in this study also prompted the selection of this material. In addition to the selection of metal materials for metal-on-metal bearings, other aspects considering the textured surface, geometric parameters, coating application, surgical procedure, ultra-precision polishing, and surface finish also need to be carried out in the future to minimize implant failures.

Author Contributions: Conceptualization, M.I.A.; methodology, M.I.A.; software, M.I.A.; validation, M.I.A.; formal analysis, M.I.A.; investigation, M.I.A.; resources, G.S., S.S. and T.S.; data curation, M.I.A.; writing—original draft preparation, M.I.A.; writing—review and editing, J.J. and E.v.d.H.; visualization, M.I.A.; supervision, J.J. and E.v.d.H.; project administration, G.S., S.S. and T.S.; funding acquisition, J.J. and E.v.d.H. All authors have read and agreed to the published version of the manuscript.

Funding: The research was funded by World Class Research UNDIP number 118-23/UN7.6.1/PP/2021.

Institutional Review Board Statement: Not applicable.

Informed Consent Statement: Not applicable.

Data Availability Statement: The data presented in this study are available on request from the corresponding author.

Acknowledgments: We gratefully thank Diponegoro University, Pasundan University and University of Twente as the authors' institutions for their strong support in our conducted research.

Conflicts of Interest: The authors declare no conflict of interest.

References

1. Savio, D.; Bagnò, A. When the Total Hip Replacement Fails: A Review on the Stress-Shielding Effect. *Processes* **2022**, *10*, 612. [[CrossRef](#)]
2. Speranza, A.; Massafra, C.; Pecchia, S.; Di Niccolo, R.; Iorio, R.; Ferretti, A. Metallic versus Non-Metallic Cerclage Cables System in Periprosthetic Hip Fracture Treatment: Single-Institution Experience at a Minimum 1-Year Follow-Up. *J. Clin. Med.* **2022**, *11*, 1608. [[CrossRef](#)]
3. Keele University. *A Guide for People Who Have Osteoarthritis*, 2014th ed.; Keele University: Staffordshire, UK, 2014.
4. Bühlhoff, M.; Zeifang, F.; Welters, C.; Renkawitz, T.; Schiltenswolf, M.; Tross, A.-K. Medium- to Long-Term Outcomes after Reverse Total Shoulder Arthroplasty with a Standard Long Stem. *J. Clin. Med.* **2022**, *11*, 2274. [[CrossRef](#)] [[PubMed](#)]
5. Solarino, G.; Carlet, A.; Moretti, L.; Miolla, M.P.; Ottaviani, G.; Moretti, B. Clinical Results in Posterior-Stabilized Total Knee Arthroplasty with Cementless Tibial Component in Porous Tantalum: Comparison between Monoblock and Two Pegs vs. Modular and Three Pegs. *Prosthesis* **2022**, *4*, 160–168. [[CrossRef](#)]

6. Arthritis Research, UK. *Hip Replacement Surgery- Patient Information*, 2011st ed.; Arthritis Research UK: Chesterfield, UK, 2011.
7. Gonzalez, R.; Muñoz-Mahamad, E.; Bori, G. One-Stage Hip Revision Arthroplasty Using Megaprosthesis in Severe Bone Loss of The Proximal Femur Due to Radiological Diffuse Osteomyelitis. *Trop. Med. Infect. Dis.* **2021**, *7*, 5. [[CrossRef](#)]
8. D’Apolito, R.; Zagra, L. Uncemented Cups and Impaction Bone Grafting for Acetabular Bone Loss in Revision Hip Arthroplasty: A Review of Rationale, Indications, and Outcomes. *Materials* **2022**, *15*, 3728. [[CrossRef](#)]
9. Yan, X.; Dong, S.; Li, X.; Zhao, Z.; Dong, S.; An, L. Optimization of Machining Parameters for Milling Zirconia Ceramics by Polycrystalline Diamond Tool. *Materials* **2021**, *15*, 208. [[CrossRef](#)]
10. Australian Orthopaedic Association National Joint Replacement Registry. *Annual Report 2020*, 2020th ed.; Australian Orthopaedic Association: Adelaide, Australia, 2020.
11. EU—Indonesia Business Network. *EIBN Sector Reports: Medical Devices*, 2018th ed.; EU—Indonesia Business Network: Jakarta, Indonesia, 2018.
12. Paluch, E.; Sobierajska, P.; Okińczyc, P.; Widelski, J.; Duda-Madej, A.; Krzyżanowska, B.; Krzyżek, P.; Ogórek, R.; Szperlik, J.; Chmielowiec, J.; et al. Nanoapatites Doped and Co-Doped with Noble Metal Ions as Modern Antibiofilm Materials for Biomedical Applications against Drug-Resistant Clinical Strains of *Enterococcus faecalis* VRE and *Staphylococcus aureus* MRSA. *Int. J. Mol. Sci.* **2022**, *23*, 1533. [[CrossRef](#)]
13. Kovac, V.; Poljsak, B.; Bergant, M.; Scancar, J.; Mezeg, U.; Primozic, J. Differences in Metal Ions Released from Orthodontic Appliances in an In Vitro and In Vivo Setting. *Coatings* **2022**, *12*, 190. [[CrossRef](#)]
14. Falisi, G.; Foffo, G.; Severino, M.; Di Paolo, C.; Bianchi, S.; Bernardi, S.; Pietropaoli, D.; Rastelli, S.; Gatto, R.; Botticelli, G. SEM-EDX Analysis of Metal Particles Deposition from Surgical Burs after Implant Guided Surgery Procedures. *Coatings* **2022**, *12*, 240. [[CrossRef](#)]
15. Ryu, J.J.; Cudjoe, E.; Patel, M.V.; Caputo, M. Sliding Corrosion Fatigue of Metallic Joint Implants: A Comparative Study of CoCrMo and Ti6Al4V in Simulated Synovial Environments. *Lubricants* **2022**, *10*, 65. [[CrossRef](#)]
16. Kumar, S.; Chandra, S.K.; Dixit, S.; Kumar, K.; Kumar, S.; Murali, G.; Vatin, N.I.; Sabri, M.M.S. Neural Network Prediction of Slurry Erosion Wear of Ni-WC Coated Stainless Steel 420. *Metals* **2022**, *12*, 706. [[CrossRef](#)]
17. Li, H.; Liang, X.; Li, Y.; Lin, F. Performance of High-Layer-Thickness Ti6Al4V Fabricated by Electron Beam Powder Bed Fusion under Different Accelerating Voltage Values. *Materials* **2022**, *15*, 1878. [[CrossRef](#)]
18. Zadrozny, L.; Czajkowska, M.; Tallarico, M.; Wagner, L.; Markowski, J.; Mijiritsky, E.; Ciccì, M. Prosthetic Surgical Templates and Dental Implant Site Time Preparation: An In Vitro Study. *Prosthesis* **2022**, *4*, 25–37. [[CrossRef](#)]
19. Orejas-Perez, J.; Gimenez-Gonzalez, B.; Ortiz-Collado, I.; Thuissard, I.J.; Santamaria-Laorden, A. In Vivo Complete-Arch Implant Digital Impressions: Comparison of the Precision of Three Optical Impression Systems. *Int. J. Environ. Res. Public Health* **2022**, *19*, 4300. [[CrossRef](#)]
20. Akbar, I.; Prakoso, A.T.; Astrada, Y.M.; Sinaga, M.S.; Ammarullah, M.I.; Adanta, D.; Mataram, A.; Syahrom, A.; Jamari, J.; Basri, H. Permeability Study of Functionally Graded Scaffold Based on Morphology of Cancellous Bone. *Malays. J. Med. Health Sci.* **2021**, *17* (Suppl. 13), 60–66.
21. Idzior-Haufa, M.; Pilarska, A.; Gajewski, T.; Szajek, K.; Faściszewski, L.; Boniecki, P.; Pilarski, K.; Łukaszewska-Kuska, M.; Dorocka-Bobkowska, B. Assessment of Contact Pressures between a Mandibular Overdenture and the Prosthodontic Area. *Appl. Sci.* **2021**, *11*, 4339. [[CrossRef](#)]
22. Shi, R.; Wang, B.; Liu, J.; Yan, Z.; Dong, L. Influence of Cross-Shear and Contact Pressure on Wear Mechanisms of PEEK and CFR-PEEK in Total Hip Joint Replacements. *Lubricants* **2022**, *10*, 78. [[CrossRef](#)]
23. Lee, H.K.; Kim, S.M.; Lim, H.S. Computational Wear Prediction of TKR with Flatback Deformity during Gait. *Appl. Sci.* **2022**, *12*, 3698. [[CrossRef](#)]
24. Jamari, J.; Ammarullah, M.; Saad, A.; Syahrom, A.; Uddin, M.; van der Heide, E.; Basri, H. The Effect of Bottom Profile Dimples on the Femoral Head on Wear in Metal-on-Metal Total Hip Arthroplasty. *J. Funct. Biomater.* **2021**, *12*, 38. [[CrossRef](#)]
25. Levanov, I.; Doykin, A.; Zadorozhnaya, E.; Novikov, R. Investigation Antiwear Properties of Lubricants with the Geo-Modifiers of Friction. *Tribol. Ind.* **2017**, *39*, 302–306. [[CrossRef](#)]
26. De la Torre, B.; Barrios, L.; De la Torre-Mosquera, J.; Bujan, J.; Ortega, M.A.; González-Bravo, C. Analysis of the Risk of Wear on Cemented and Uncemented Polyethylene Liners According to Different Variables in Hip Arthroplasty. *Materials* **2021**, *14*, 7243. [[CrossRef](#)] [[PubMed](#)]
27. Jamari, J.; Ammarullah, M.I.; Santoso, G.; Sugiharto, S.; Supriyono, T.; Prakoso, A.T.; Basri, H.; van der Heide, E. Computational Contact Pressure Prediction of CoCrMo, SS 316L and Ti6Al4V Femoral Head against UHMWPE Acetabular Cup under Gait Cycle. *J. Funct. Biomater.* **2022**, *13*, 64. [[CrossRef](#)] [[PubMed](#)]
28. Ammarullah, M.I.; Afif, I.Y.; Maula, M.I.; Winarni, T.I.; Tauviqirrahman, M.; Bayuseno, A.P.; Basri, H.; Syahrom, A.; Saad, A.P.M.; Jamari, J. 2D Computational Tresca Stress Prediction of CoCrMo-on- UHMWPE Bearing of Total Hip Prosthesis Based on Body Mass Index. *Malays. J. Med. Health Sci.* **2021**, *17* (Suppl. 13), 18–21.
29. Handoko; Suyitno; Rini, D.; Magetsari, R. Numerical Convergence in Wear Volume Prediction of UHMWPE Acetabular Cup Paired with cp Ti Femoral Head Hip Implants. *Key Eng. Mater.* **2020**, *867*, 148–158. [[CrossRef](#)]
30. Ammarullah, M.I.; Afif, I.Y.; Maula, M.I.; Winarni, T.I.; Tauviqirrahman, M.; Jamari, J. Tresca stress evaluation of Metal-on-UHMWPE total hip arthroplasty during peak loading from normal walking activity. *Mater. Today Proc.* **2022**, *63*, S143–S146. [[CrossRef](#)]

31. Ammarullah, M.I.; Afif, I.Y.; Maula, M.I.; Winarni, T.I.; Tauviqirrahman, M.; Akbar, I.; Basri, H.; van der Heide, E.; Jamari, J. Tresca Stress Simulation of Metal-on-Metal Total Hip Arthroplasty during Normal Walking Activity. *Materials* **2021**, *14*, 7554. [[CrossRef](#)]
32. Ammarullah, M.I.; Santoso, G.; Sugiharto, S.; Supriyono, T.; Kurdi, O.; Tauviqirrahman, M.; Winarni, T.I.; Jamari, J. Tresca Stress Study of CoCrMo-on-CoCrMo Bearings Based on Body Mass Index Using 2D Computational Model. *J. Tribol.* **2022**, *33*, 31–38.
33. Basri, H.; Syahrom, A.; Ramadhoni, T.S.; Prakoso, A.T.; Ammarullah, M.I.; Vincent. The analysis of the dimple arrangement of the artificial hip joint to the performance of lubrication. *IOP Conf. Ser. Mater. Sci. Eng.* **2019**, *620*, 012116. [[CrossRef](#)]
34. Yin, H.; Bai, X.; Fu, H. Prediction of Work Hardening in Bearing Steels Undergoing Rolling Contact Loading with a Dislocation-Based Model. *Metals* **2022**, *12*, 555. [[CrossRef](#)]
35. Dassault Systèmes. *Abaqus Analysis User's Guide Volume IV: Elements*; Dassault Systèmes Simulia Corp.: Providence, RI, USA, 2016.
36. Bohdal, L.; Kukielka, L.; Patyk, R.; Koška, K.; Chodór, J.; Czyżewski, K. Experimental and Numerical Studies of Tool Wear Processes in the Nibbling Process. *Materials* **2021**, *15*, 107. [[CrossRef](#)] [[PubMed](#)]
37. Wang, C.; Pek, J.X.; Chen, H.M.; Huang, W.M. On-Demand Tailoring between Brittle and Ductile of Poly(methyl methacrylate) (PMMA) via High Temperature Stretching. *Polymers* **2022**, *14*, 985. [[CrossRef](#)] [[PubMed](#)]
38. Borawski, A. Testing Passenger Car Brake Pad Exploitation Time's Impact on the Values of the Coefficient of Friction and Abrasive Wear Rate Using a Pin-on-Disc Method. *Materials* **2022**, *15*, 1991. [[CrossRef](#)] [[PubMed](#)]
39. Vara, J.C.; Delgado, J.; Estrada-Martínez, A.; Pérez-Pevida, E.; Brizuela, A.; Bosch, B.; Pérez, R.; Gil, J. Effect of the Nature of the Particles Released from Bone Level Dental Implants: Physicochemical and Biological Characterization. *Coatings* **2022**, *12*, 219. [[CrossRef](#)]
40. Ammarullah, M.I.; Afif, I.Y.; Maula, M.I.; Winarni, T.I.; Tauviqirrahman, M.; Bayuseno, A.P.; Basri, H.; Syahrom, A.; Saad, A.P.M.; Jamari. Wear analysis of acetabular cup on metal-on-metal total hip arthroplasty with dimple addition using finite element method. *AIP Conf. Proc.* **2022**, *2391*, 020017. [[CrossRef](#)]
41. Utomo, M.S.; Asmaria, T.; Malau, D.P.; Triwardono, J.; Kartika, I.; Dologo, I.H.; Rahyussalim, A.J. Design criteria for cementless total hip arthroplasty: A retrospective study from cadaver implantation. *AIP Conf. Proc.* **2021**, *2344*, 020019. [[CrossRef](#)]
42. Maistrovskaia, Y.V.; Nevzorova, V.A.; Ugay, L.G.; Gnedenkov, S.V.; Kotsurbei, E.A.; Moltyh, E.A.; Kostiv, R.E.; Sinebryukhov, S.L. Bone Tissue Condition during Osteosynthesis of a Femoral Shaft Fracture Using Biodegradable Magnesium Implants with an Anticorrosive Coating in Rats with Experimental Osteoporosis. *Appl. Sci.* **2022**, *12*, 4617. [[CrossRef](#)]
43. London Health Sciences Centre. *My Guide to Total Hip Joint Replacement*, 2013rd ed.; London Health Sciences Centre: London, UK, 2013.
44. Fan, Z.; Tian, Y.; Zhou, Q.; Shi, C. Enhanced magnetic abrasive finishing of Ti-6Al-4V using shear thickening fluids additives. *Precis. Eng.* **2020**, *64*, 300–306. [[CrossRef](#)]
45. Fan, Z.; Tian, Y.; Liu, Z.; Shi, C.; Zhao, Y. Investigation of a novel finishing tool in magnetic field assisted finishing for titanium alloy Ti-6Al-4V. *J. Manuf. Process.* **2019**, *43*, 74–82. [[CrossRef](#)]
46. Fan, Z.; Tian, Y.; Zhou, Q.; Shi, C. A magnetic shear thickening media in magnetic field-assisted surface finishing. *Proc. Inst. Mech. Eng. Part B J. Eng. Manuf.* **2020**, *234*, 1069–1072. [[CrossRef](#)]
47. Tian, Y.; Shi, C.; Fan, Z.; Zhou, Q. Experimental investigations on magnetic abrasive finishing of Ti-6Al-4V using a multiple pole-tip finishing tool. *Int. J. Adv. Manuf. Technol.* **2020**, *106*, 3071–3080. [[CrossRef](#)]
48. Wang, M.; Yang, W.; Cui, H.; Yang, S.-C.; Liu, Z.-N.; Lu, G.-L. Theoretical Investigation on the Friction Behavior of Bio-Inspired Hard-Soft-Integrated Materials. *Coatings* **2021**, *11*, 1296. [[CrossRef](#)]
49. Abdel-Jaber, M.; Abdel-Jaber, M.S.; Beale, R.G. An Experimental Study into the Behaviour of Tube and Fitting Scaffold Structures under Cyclic Side and Vertical Loads. *Metals* **2021**, *12*, 40. [[CrossRef](#)]
50. Ammarullah, M.I.; Afif, I.Y.; Maula, M.I.; Winarni, T.I.; Tauviqirrahman, M.; Bayuseno, A.P.; Basri, H.; Syahrom, A.; Saad, A.P.M. Jamari Deformation analysis of CoCrMo-on-CoCrMo hip implant based on body mass index using 2D finite element procedure. *J. Phys. Conf. Ser.* **2022**, *2279*, 012004. [[CrossRef](#)]